

# Comparative Performance Analysis of Sharpbelly Fish and Equilibrium Optimizers for Green Economic Load Dispatch Considering Prohibited Operating Zones and Multiple Fuel Constraints

Do Huynh Thanh<sup>1</sup>Phong and Nguyen Thuy Linh<sup>2\*</sup>

Faculty of electrical & electronics engineering, Ly Tu Trong College, Ho Chi Minh city, Vietnam Email: [nguyenthuylinh@ltdc.edu.vn](mailto:nguyenthuylinh@ltdc.edu.vn)



Published in  
VOI- 2 Issue: 3

DOI:10.5281/zenodo.20259560

PP: 10-23

\*Correspondence:

**Nguyen Thuy Linh**  
Faculty of electrical &  
electronics engineering, Ly Tu  
Trong College, Ho Chi Minh  
city, Vietnam Email:  
[nguyenthuylinh@ltdc.edu.vn](mailto:nguyenthuylinh@ltdc.edu.vn)

## Abstract

*This study investigates the Green Economic Load Dispatch (GELD) problem, focusing on the integration of renewable energy into traditional thermal grids. We evaluate and compare the performance of two meta-heuristic algorithms: the Sharpbelly Fish Optimizer (SFO) and the Equilibrium Optimizer (EO), under realistic non-convex constraints. The methodology is validated on two distinct scenarios: a 6-unit thermal system incorporating prohibited operational zones, and a 10-unit system considering multi-fuel constraints alongside 100 MW of wind generation. Comparative results indicate a scale-dependent performance divergence. While EO shows high reliability in smaller configurations, SFO exhibits superior exploration and faster convergence as system dimensionality increases, resulting in more significant fuel cost reductions. These findings offer a practical framework for optimizing hybrid energy portfolios and highlight the efficacy of swarm intelligence in achieving low-carbon power dispatch.*

**Keywords:** Economic Load Dispatch; Sharpbelly Fish Optimizer; Equilibrium Optimizer; Non-Convex Optimization; Metaheuristic Algorithms; Power System Optimization.

## Introduction

The economic load dispatch (ELD) problem has long been regarded as a fundamental and critical task in the efficient operation of modern power systems [1]. Traditionally, ELD solutions focused on optimally distributing the generation output among thermal power plants (TPPs) — predominantly fossil-fuel-based units — to satisfy the system load demand at minimum total generation cost, subject to operational and system constraints [2]. Nevertheless, growing concerns over greenhouse gas emissions and their adverse effects on public health and ecological systems have prompted a paradigm shift in power system planning and operation [3]. As a result, the integration of green energy sources (GESs), particularly wind and solar photovoltaic generation, into the existing grid infrastructure has gained substantial momentum. Such integration not only contributes to a cleaner environment but also yields notable economic benefits by reducing dependence on costly fossil-fuel-based generation [4]. Consequently, the conventional ELD framework has been extended to accommodate renewable energy sources (RESs), giving rise to the green economic load dispatch (GELD) problem [5].

The GELD problem is inherently nonlinear in nature, rendering it a highly complex optimization challenge. Conventional gradient-based and deterministic iterative techniques [6–7] are widely recognized as inadequate for reliably identifying global optimal solutions, particularly in large-scale power systems comprising numerous TPPs with heterogeneous and non-convex operating characteristics. This limitation has driven increasing demand for more powerful and flexible optimization frameworks. Meta-heuristic algorithms, owing to their population-based search mechanisms and strong global exploration capabilities, have emerged as highly effective tools for addressing such complex problems. Motivated by this, a substantial body of literature has applied diverse meta-heuristic strategies to solve both ELD and GELD problems, including the Growth Optimizer Algorithm (GOA) [8], artificial bee colony algorithm (ABC) [9], turbulent flow of water algorithm (TFW) [10], Krill Herd Algorithm (KHA) [11], memetic sine cosine algorithm (MSC) [12], Stochastic Shaking Algorithm (SSA) [13], osprey optimization algorithm (OOA) [14], clustering cuckoo search (CCS) [15], Jaya Algorithm (JA) [16], multiswarm statistical particle swarm optimization (MS-PSO) [17], grasshopper optimization algorithm (GrOA) [18], Dandelion Optimizer (DO) [19], improved mayfly optimization algorithm (IMOA) [20], enhanced emperor penguin optimization (EEPO) [21], five phases algorithm (FPA) [22], Greylag Goose Optimization (GGO) [23] and the Elk Herd Optimizer (EHO) [24]. Beyond these, comparative evaluations of emerging algorithms — such as Starfish Optimization, Sand Cat Swarm Optimization, Weighted Average Algorithm (WAA), and Mirage Search Optimization — have further enriched the understanding of algorithmic behavior across complex benchmark landscapes [25]. Recent studies have highlighted the importance of advanced control strategies and system reliability in modern power systems. Hybrid control methods combining hysteresis current control and SPWM have shown improved dynamic response and reduced oscillations in electric drive applications [26]. In addition, fault-tolerant control techniques based on observer and reconfiguration strategies have been developed to maintain stable operation under sensor failures [27]. These developments indicate that effective ELD and GELD solutions require not only efficient optimization algorithms but also reliable control and resilient system operation.

This study evaluates the performance of two recent meta-heuristics— Sharpbelly Fish Optimizer (SFO) [28] and Equilibrium Optimizer (EO) [29] —in solving the Economic Load Dispatch (ELD) problem. While EO utilizes a mass balance framework and an 'equilibrium pool' to stabilize its search trajectory, SFO simulates collective fish dynamics through adaptive strategies to maintain population diversity. These algorithms are implemented to optimize power dispatch for 6-unit and 10-unit thermal systems, aiming to minimize total generation costs. To reflect a realistic modern energy landscape, the model further integrates 100 MW of wind generator (WG), providing a comparative analysis that remains largely unexplored in existing literature.

The primary contributions of this work are summarized as follows:

- Implementation of EO and SFO for large-scale optimization: The primary goal is to find the most efficient power dispatch settings for two distinct scenarios: an initial 6-unit thermal system constrained by prohibited operating zones, and an expanded 10-unit setup that accounts for complex fuel limitations.
- Modeling of Green Economic Load Dispatch (GELD): Integrating wind and solar energy into the optimization framework and quantifying their impact on reducing total production costs compared to conventional scenarios.
- Rigorous performance benchmarking: Conducting a comparative analysis based on accuracy, convergence speed, and stability to identify the most robust algorithm for complex power grids.

- Practical roadmap for renewable integration: Providing a technical reference and strategic framework for incorporating volatile renewable sources into modern grid infrastructures.

## 1. Problem formulation

### 1.1. Objective function

The main objective of this study is to minimize the total generation cost (TGC) of all thermal power plants (TPPs) in the considered power system. The TGC is formulated as [4]:

$$\begin{aligned} \text{Min } TGC = & \sum_{g=1}^{N_{gen}} a_g + b_g \times PO_g + c_g \times PO_g^2 \\ & \text{with } g = 1, \dots, N_{gen} \end{aligned} \quad 1)$$

where, TGC is the total generation cost of all thermal generators in the system;  $a_g$ ,  $b_g$ , and  $c_g$  are the cost coefficients of generator  $g$ ;  $PO_g$  is the power output of generator  $g$ ;  $N_{gen}$  is the total number of generators.

### 1.2. Fitness function

As introduced previously, the optimization problem in this study is solved using a metaheuristic algorithm, where a fitness function is evaluated throughout the search process. The fitness function is composed of the objective function defined in Eq. (1) and an additional penalty term, expressed as:

$$FV_s = TGC_s + \lambda \times Pen_s \quad 2)$$

where  $FV_s$  is the fitness value of solution  $s$ , with  $s = 1, 2, \dots, N_{sol}$  and  $N_{sol}$  denotes the total number of candidate solutions;  $TGC_s$  is the total generation cost corresponding to solution  $s$ ;  $\lambda$  is the penalty coefficient;  $Pen_s$  represents the penalty value associated with constraint violations.

### 1.3. The involved constraints

- **Multiple Fuel Constraints of Thermal Power Plants**

As mentioned earlier, this research will evaluate the multiple fuel constraint of each TPP, and the mathematical expression of the constraint is given below:

$$TFC = \begin{cases} a_{g,1} + b_{g,1} \times PO_g + c_{g,1} \times PO_g^2; & \text{if } PO_g^{1,low} \leq PO_g \leq PO_g^{1,high} \\ a_{g,2} + b_{g,2} \times PO_g + c_{g,2} \times PO_g^2; & \text{if } PO_g^{2,low} \leq PO_g \leq PO_g^{2,high} \\ \dots & \dots \\ a_{g,v} + b_{g,v} \times PO_g + c_{g,v} \times PO_g^2; & \text{if } PO_g^{v,low} \leq PO_g \leq PO_g^{v,high} \end{cases} \quad 2)$$

Where  $a_{g,1}$ ,  $b_{g,1}$  and  $c_{g,1}$  denote the fuel cost coefficients of TPP  $g$  operating with fuel type 1. The terms  $PO_g^{1,low}$  and  $PO_g^{1,high}$  represent the minimum and maximum power generation limits of unit  $g$  under the first fuel option, respectively. Likewise,  $a_{g,2}$ ,  $b_{g,2}$  and  $c_{g,2}$  correspond to the fuel cost coefficients associated with fuel type 2, while  $PO_g^{2,low}$  and  $PO_g^{2,high}$  indicate the corresponding lower and upper operating limits. In general, for fuel type  $v$ , the coefficients  $a_{g,v}$ ,  $b_{g,v}$  and  $c_{g,v}$  describe the fuel cost characteristics of TPP  $g$ ,

whereas  $PO_g^{v,low}$  and  $PO_g^{v,high}$  define the minimum and maximum output power levels achievable when unit  $g$  operates using fuel type  $v$ . Here,  $v$  denotes the index of the available fuel types.

- **The prohibited operational zone constraint**

The mathematical model of the prohibited operational zone constraint (POZ) is formulated as follows:

$$PO_{TPP,g} \in \begin{cases} PO_{TPP,g}^{low} \leq PO_{TPP,g} \leq PO_{TPP,g,1}^l \\ PO_{TPP,g,z-1}^u \leq PO_{TPP,g} \leq PO_{TPP,g,z}^l; z = 2, \dots, n_i; \forall z \in \Omega \\ PO_{TPP,g,n_i}^u \leq PO_{TPP,g} \leq PO_{TPP,g}^{high} \end{cases} \quad (3)$$

Where,  $PO_{TPP,g,1}^l$  is the lower boundary of power output of the  $1$ th prohibited zone;  $PO_{TPP,g,z-1}^u$  is the upper boundary of power output of the  $(z-1)$ th prohibited zone with  $z = 1, 2, \dots, n_i$  and  $n_i$  is the number of the POZs of the TPPs;  $PO_{TPP,g,z}^l$  is the lower boundary of power output of the  $z$ th prohibited zone;  $PO_{TPP,g,n_i}^u$  is the upper boundary of power output of the  $n_i$ th;

- **Power balance constraint:**

This constraint ensures that the total generated power from all available sources matches the system demand, including transmission losses. It can be expressed as [30]:

$$\sum_{g=1}^{N_{gen}} PO_g + \sum_{l=1}^{N_{OWU}} PO_{OWU,w} + \sum_{r=1}^{N_{OSU}} PO_{OSU,s} = PO_D + PO_L \quad (4)$$

where  $\sum_{g=1}^{N_{gen}} PO_g$  is the total power produced by thermal generators;  $PO_{OWU}$  is the power output of wind units, respectively;  $PO_D$  denotes the total power output required by the load demand;  $PO_L$  signifies the total power output loss due to transmission line characteristics.

The transmission loss in Eq. (4) is calculated using the following quadratic form [31]:

$$PO_L = \sum_{g=1}^{N_{gen}} \sum_{h=1, g \neq h}^{N_{gen}} PO_g \times LP_{gh} \times PO_h + \sum_{g=1}^{N_{gen}} LP_{0g} \times PO_g + LP_{00} \quad (5)$$

where,  $LP_{gh}$ ,  $LP_{g0}$ , and  $LP_{00}$  are the network loss parameters.

- **Generator operating limits:**

This constraint ensures that the output power of each thermal generator remains within its allowable operating range [32],[33]:

$$PO_g^{min} \leq PO_g \leq PO_g^{max} \quad (6)$$

where,  $PO_g^{min}$  and  $PO_g^{max}$  are the minimum and maximum power output limits of generator  $g$ ;  $PO_g$  the actual power output of generator  $g$ .

- **Wind generation limits**

As mentioned earlier, this research integrates a 100 MW wind generator in both systems. The power output of a wind generator is restricted by its technical capabilities [34 - 36]:

$$PO_{WG}^{min} \leq PO_{WG} \leq PO_{WG}^{max} \quad 7)$$

where  $PO_{WG}^{min}$  and  $PO_{WG}^{max}$  are the minimum and maximum of power output of the WG ;  $PO_{WG}$  is the power output by the WG.

## 2. Applied algorithms

### 2.1. Sharpbelly Fish Optimizer (SFO)

#### 2.1.1. Velocity calculation

At each iteration, the position of every solution is updated through a composite velocity that integrates four distinct behavioral components: directional movement, collective aggregation, random perturbation, and reinitialization. Each component targets a specific challenge in balancing exploration and exploitation during the search process. Solutions are naturally inclined to drift toward regions of the search space that have already shown higher quality.

The movement velocity for each solution is computed as follows:

$$V_i^{move} = w_i \times rand \times (P_{best} - P_i) \quad 8)$$

$$w_i = 1 - \frac{F_{P_i}}{\max(\sum_{i=1}^{Npz} F_{P_i}) + \delta} \quad 9)$$

where  $V_i^{move}$  is the displacement vector of the  $i$ -th solution at iteration  $m$ , and  $w_m$  is an adaptive weight that reflects the solution's relative performance within the current population.  $P_{best}$  the global best solution;  $P_i$  the current position with  $i = 1, 2, \dots, Npz$  with  $Npz$  is the population size;  $F_{P_i}$  is the fitness value of the current solution;  $\max(\sum_{i=1}^n F_{P_i})$  is the worst fitness value across all solutions at current iteration, which serves as a normalization reference for scaling individual movement rates. The small constant  $\delta > 0$  is included to prevent any numerical instability caused by division by zero.

The aggregation velocity is formulated as:

$$V_i^{agg} = \beta \times rand \times (P_{best} - P_i) \quad 10)$$

where  $V_i^{agg}$  denotes the aggregation velocity of the  $i$ -th solution, directing it toward the global best position  $P_{best}$ . The coefficient  $\beta \in (0,1)$  governs the intensity of this attraction, allowing the algorithm to maintain a consistent exploitative pressure across all solutions regardless of their individual fitness levels.

The perturbation velocity for each solution is defined as:

$$V_i^{perturb} = \begin{cases} \sigma \times RV, & \text{if } r < P_q \\ 0, & \text{otherwise} \end{cases} \quad 11)$$

where  $V_i^{perturb}$  is the perturbation displacement applied to the  $i$ -th solution,  $RV$  denotes a standard Gaussian random vector, and  $r$  is a uniformly drawn random number compared against the activation

threshold  $P_q \in [0,1]$ . The scaling factor  $\sigma$  controls how large the perturbation step can be. A larger value of  $P_q$  increases the frequency of random disruptions, which benefits exploration, while a smaller value keeps the search more focused and stable around promising regions.

The reinitialization velocity is formulated as:

$$V_i^{reinit} = \begin{cases} \lambda \times (2 \times rand - 1) \times (b_{up} - b_{low}), & \text{if } k_{stag} \geq T_p \\ 0, & \text{otherwise} \end{cases} \quad (12)$$

where  $V_i^{reinit}$  represents the reinitialization step applied to solution  $m$  when stagnation is confirmed. The counter  $k_{stag}$  tracks how many consecutive iterations have passed without improvement in the best objective value. Once  $k_{stag}$  reaches the patience threshold  $T_p$ , the affected solution is relocated by a random vector scaled by  $\lambda \in [0,1]$ , which determines the extent of the repositioning within the search bounds  $b_{up}$ ;  $b_{low}$ . This mechanism effectively prevents the population from clustering prematurely and helps the algorithm recover from local optima.

### 2.1.2. Position Update

At each iteration, the total displacement of every solution is obtained by summing all active velocity components generated by the mechanisms described in the previous subsections:

$$V_i = V_i^{move} + V_i^{agg} + V_i^{perturb} + V_i^{reinit} \quad (13)$$

Where  $V_i$  the total velocity of the solution  $ith$ .

Once the composite velocity is determined, the new position of the  $ith$  solution is updated using the following expression:

$$P_i^{new} = P_i + V_i \quad (14)$$

Where  $P_i^{new}$  is the new position of the  $ith$  solution;

To maintain feasibility throughout the search, every updated position is immediately clipped back into the allowable search domain using a simple boundary-handling operation:

$$P_i^{new} = \min(\max(P_i^{new}, b_{low}), b_{up}) \quad (15)$$

After the new solutions are fully determined and checked for their violation of the search space, the refining procedure will commence using the following expression:

$$P_i^{new} = \begin{cases} P_i^{new}, & \text{if } F_{P_i^{new}} < F_{P_{Best}} \\ P_{best}, & \text{otherwise} \end{cases} \quad (16)$$

Where  $F_{P_i^{new}}$  is the fitness value of the new position;

## 2.2. Equilibrium Optimizer (EO)

The initial set of equilibrium candidate solutions is constructed by uniformly distributing particles across the search space as follows:

$$P_i = P_i^{low} + \rho_1 \times (P_i^{high} - P_i^{low}) \quad (17)$$

Where  $\rho_1$  is a random value in the interval of zero and 1.

The equilibrium reservoir  $P^{res}$  is subsequently constituted from the four highest-ranked candidate solutions identified within the current population, augmented by their arithmetic mean, as expressed below:

$$P^{res} = [P_{(1)}; P_{(2)}; P_{(3)}; P_{(4)}; P_{(Mean)}] \quad (18)$$

At each iteration, a new candidate solution  $P_i^{new}$  is derived by combining the current candidate  $P_i$  with a randomly selected member  $P^{res}$  drawn from the equilibrium pool, governed by the following update rule:

$$P_i^{new} = P_{R1}^{res} + (P_i - P_{R1}^{res}) \times \beta + \frac{\gamma}{Sv \times V} \times (1 - F) \quad (19)$$

In this formulation,  $\beta$  is a balancing factor that regulates the trade-off between global exploration and local exploitation;  $\gamma$  denotes the generation rate, which constitutes the most critical component of the proposed algorithm as it governs the intensification of the exploitation phase to enhance solution accuracy;  $Sv$  is a stochastic vector sampled uniformly from  $[0, 1]$ ;  $F$  is the exponential term;  $V$  is the initial control volume.

The auxiliary parameters are defined as follows:

$$\beta = \alpha_1 \times \text{sign}(\text{rand} - 0.5) \times (e^{-\lambda d} - 1) \quad (20)$$

$$\gamma = \gamma_0 \times F \quad (21)$$

$$G_0 = GCP \times (P_{R1}^{res} - \lambda \times P_i) \quad (22)$$

$$GCP = \begin{cases} 0.5 \times \text{Rand1} & \text{rand2} \geq GP \\ 0 & \text{rand2} < GP \end{cases} \quad (23)$$

where  $P^g$  represents the generation probability threshold

$$d = \left(1 - \frac{t}{t_{max}}\right)^{(\alpha_2 \times \frac{t}{t_{max}})} \quad (24)$$

In Eq. (24),  $t$  denotes the current iteration index and  $t_{max}$  is the maximum number of iteration index, while  $\alpha_1$  and  $\alpha_2$  are algorithm-specific control constants.

### 3. Results and discussions

To evaluate the performance of the proposed methodologies, both the Sharpbelly Fish Optimizer and the Equilibrium Optimizer were implemented within the MATLAB 2018a environment. The computational simulations were conducted on a workstation powered by an Intel(R) Core(TM) i7-14700 processor (2.10 GHz) and 32 GB of RAM. This hardware configuration was chosen to ensure high processing speeds and the consistency of the numerical results. In this study, the practical effectiveness of the algorithms was validated across two distinct test systems. The first system consists of 6 thermal units incorporating the prohibited operational zone constraint, while the second is scaled up to 10 units considering multiple fuel constraints. The inclusion of the 10-unit system serves to assess the algorithms' optimization capabilities when dealing with increased complexity and higher-dimensional search spaces.

### 3.1. The results obtained on the first system

To test how reliable the proposed methods are, 50 independent runs were carried out, with results shown in Figure 1. SFO proved unstable — its fitness values varied widely across trials, suggesting it often gets stuck in local optima. EO, on the other hand, was much more consistent, repeatedly finding good solutions at a lower average cost. This makes EO the stronger choice for exploring the search space and finding high-quality solutions. Figure 2 compares how SFO and EO converge over 100 iterations using minimum, average, and maximum fitness values. SFO drops quickly at first but tends to level off early, getting trapped in suboptimal areas. EO keeps improving throughout, balancing exploration and exploitation more effectively and reaching better final solutions. Figure 3 shows the statistical values of TGC achieved by SFO and EO through the three criteria including the Minimum TGC (Min TGC), Mean TGC (Mean TGC), and Maximum TGC (Max TGC). The most notable gaps are in Mean and Max fuel costs, where EO saves \$0.23/h and \$0.75/h, respectively. Its STD of 0.0033 is also two orders of magnitude smaller than SFO's (0.2013), meaning EO behaves far more predictably. Over long operating schedules, these savings add up significantly, making EO a practical and reliable option for large-scale power system optimization.

Figure 4 shows how power is distributed across six thermal units (ThU 1–6) for both SFO and EO. The two algorithms produce very similar profiles. ThU 1 handles the largest share of the load at around 527.9 MW. Small differences appear in ThU 3 and ThU 6 — where SFO slightly reduces ThU 1's load and makes up for it with a higher output from ThU 6. Overall, the results are closely matched, showing that both SFO and EO can find valid, high-quality dispatch solutions within the given constraints.

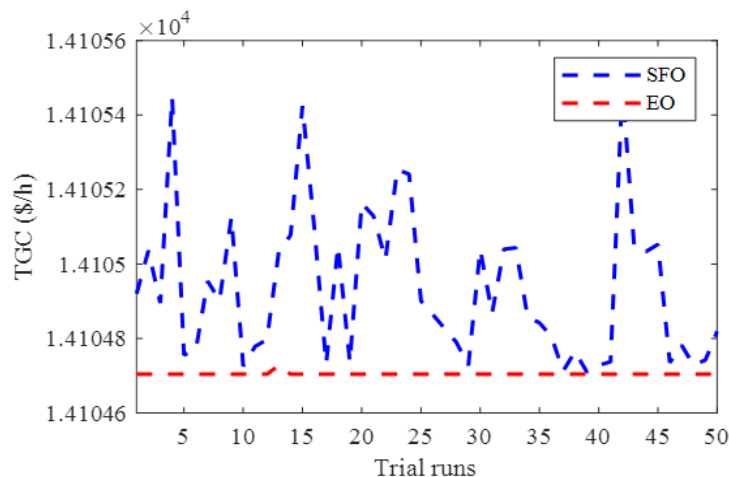


**Figure 1. Fuel cost distribution of SFO and EO over 50 independent runs for the 6-unit test system**

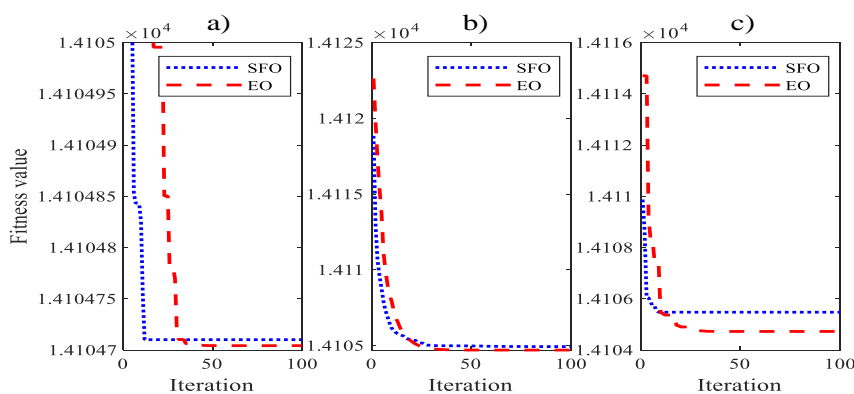


**Figure 2. Convergence profiles of SFO and EO for (a) min, (b) mean, and (c) max fitness values on the 6-unit test system.**

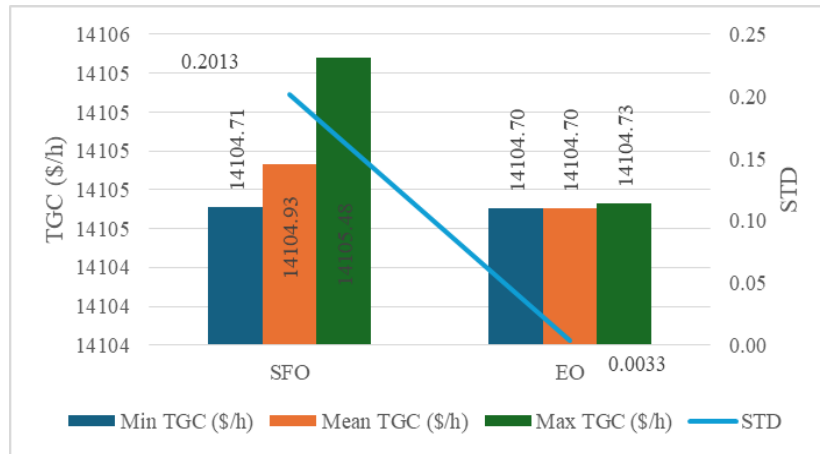


**Figure 3. Statistical performance comparison of SFO and EO on the 6-unit test system.**

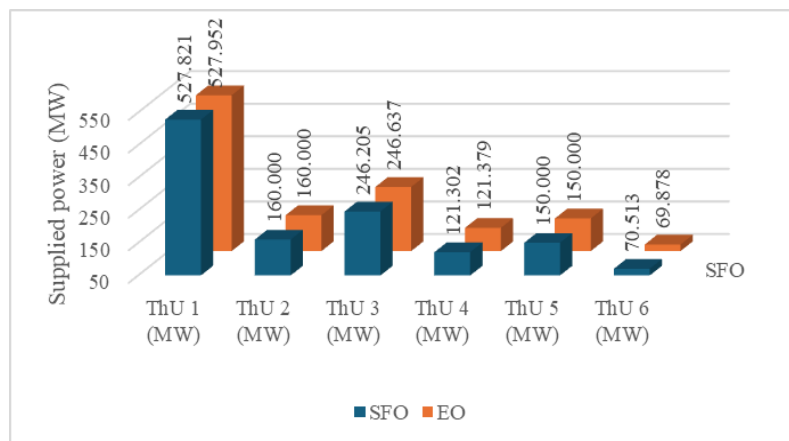
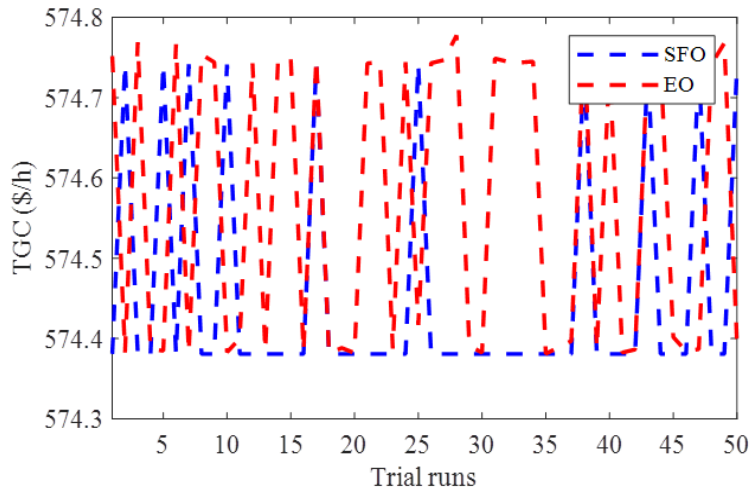


**Figure 4. Optimal power dispatch of thermal units obtained by SFO and EO for the 6-unit test system.**

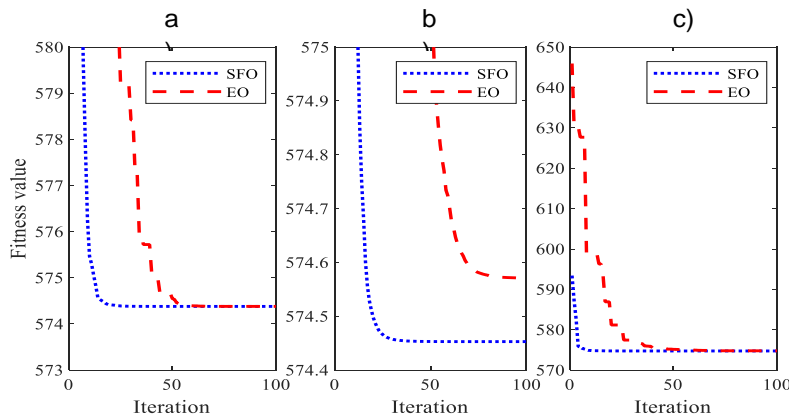
### 1.1. The results obtained on the second system

Figure 5 shows the stochastic performance of SFO and EO over 50 independent trials. SFO proved to be highly consistent, staying close to the global optimum with very little variance across all runs. EO, however, was more sensitive to initial conditions, leading to larger fluctuations and a standard deviation of 0.1833. This instability makes EO less reliable for complex power dispatch problems. SFO's steady results and lower average costs show it handles the randomness of metaheuristic search much better. The convergence curves in Figure 6 tell a similar story. SFO descended much faster in the early stages and reached a stable plateau well before EO, showing it has a strong exploitation mechanism that finds better solutions in fewer iterations. Both methods eventually approach the global minimum, but SFO consistently maintains a lower fitness level throughout. This confirms SFO as the more efficient and dependable option for this problem. Figure 7 compares both algorithms across four key metrics. Both achieve the same Minimum Fuel Cost (\$574.381/h), but SFO pulls ahead in everything else — a lower Mean Fuel Cost of \$574.453/h, a reduction in Maximum Fuel Cost by \$0.036/h, and a Standard Deviation of 0.1457 compared

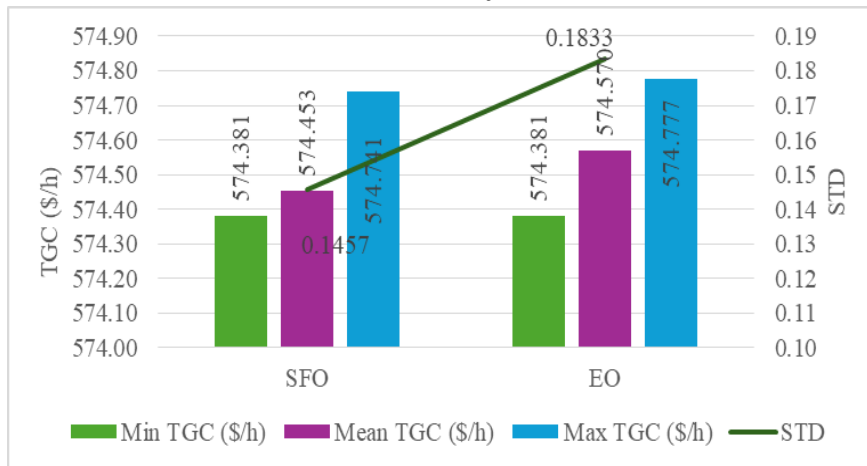
to EO's 0.1833, a difference of 0.0376. SFO not only delivers better economics but also more consistent, predictable results. Figure 8 shows the power output across ten thermal units (ThU 1–10) in MW. ThU 9 and ThU 10 carry the heaviest loads, while ThU 2 contributes the least. SFO's power distributions and fuel costs closely match those of EO, which shows that SFO can handle complex engineering constraints just as effectively.



**Figure 5. Fuel cost distribution of SFO and EO over 50 independent runs for the 10-unit test system**



**Figure 6. Convergence profiles of SFO and EO for (a) min, (b) mean, and (c) max fitness values on the 10-unit test system.**



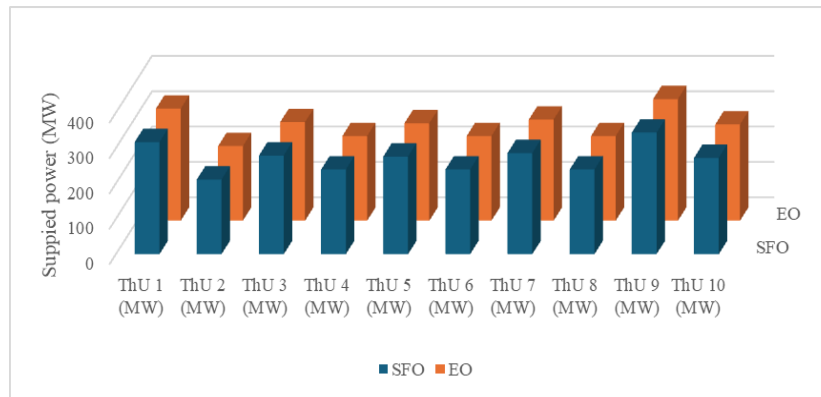


Figure 8. Optimal power dispatch of thermal units obtained by SFO and EO for the 10-unit test system.

#### 4. Conclusion

This study has successfully developed and implemented a robust optimization framework for the Green Economic Load Dispatch (GELD) problem, integrating renewable energy sources with traditional thermal power plants. Through the application of two advanced meta-heuristic algorithms—the Equilibrium Optimizer (EO) and the Sharpbelly Fish Optimizer (SFO)—this research provides a detailed benchmark of their performance in handling non-convex constraints such as valve-point effects and prohibited operational zones. The experimental results demonstrate that both algorithms offer high-quality solutions; however, their efficacy varies with system complexity. EO proved to be highly reliable in smaller-scale configurations, maintaining remarkable statistical stability and minimal standard deviation across multiple trials. In contrast, SFO demonstrated a superior ability to navigate high-dimensional search spaces as the system expanded to include more thermal units and significant renewable penetration. The integration of 100 MW wind sources not only reduced total generation costs but also highlighted the potential for substantial carbon footprint reduction in modern grid operations. The primary contribution of this work lies in the direct comparative validation of these two state-of-the-art algorithms, providing empirical evidence for their selection in large-scale power system planning. Despite the positive outcomes, this study faces certain limitations. The current model assumes static load demands and does not fully account for the inherent intermittency of solar and wind generation in real-time scenarios. Furthermore, the optimization focuses primarily on economic cost, without a detailed multi-objective analysis of emission levels. Future research will focus on expanding this framework to include dynamic environmental economic dispatch (DEED) and considering the stochastic nature of renewable energy through probabilistic modeling. Additionally, hybridizing EO and SFO to leverage their respective strengths in stability and exploration could potentially yield even more efficient tools for the next generation of smart grid management.

#### References

1. Mohammadi, F., & Abdi, H. (2018). A modified crow search algorithm (MCSA) for solving economic load dispatch problem. *Applied Soft Computing*, 71, 51-65.
2. Pham, L. H., Nguyen, T. T., Pham, L. D., & Nguyen, N. H. (2019). Stochastic fractal search based method for economic load dispatch. *TELKOMNIKA (Telecommunication Computing Electronics and Control)*, 17(5), 2535-2546.

3. Singh, N., Chakrabarti, T., Chakrabarti, P., Margala, M., Gupta, A., Praveen, S. P., ...&Unhelkar, B. (2023). Novel heuristic optimization technique to solve economic load dispatch and economic emission load dispatch problems. *Electronics*, 12(13), 2921.
4. Nguyen, V. U. P., Minh, H. H., & Nguyen, T. T. (2024). Optimal renewable-integrated economic load dispatch for a large-scale power system using One-to-One Optimization Algorithm. *Journal of Advanced Engineering and Computation*, 8(1), 9-18.
5. Nguyen, V.U.P. & Nguyen, T.D. (2026). Minimizing the overall electricity production cost to the large-scale power system incorporating solar and wind energy sources using Elk Herd Optimizer. *Journal of Advanced Engineering and Computation*, Vol. 10, Iss. 1, pp. 36–49. DOI: 10.55579/jaec.2026101.523
6. Nanda, J., Hari, L., & Kothari, M. L. (1994). Economic emission load dispatch with line flow constraints using a classical technique. *IEE Proceedings-Generation, Transmission and Distribution*, 141(1), 1-10.
7. Farag, A., Al-Baiyat, S., & Cheng, T. C. (1995). Economic load dispatch multiobjective optimization procedures using linear programming techniques. *IEEE Transactions on Power systems*, 10(2), 731-738.
8. Shaban, A. E., Ismaeel, A. A., Farhan, A., Said, M., & El-Rifaie, A. M. (2024). Growth Optimizer Algorithm for Economic Load Dispatch Problem: Analysis and Evaluation. *Processes*, 12(11), 2593.
9. Abu-Mouti, F. S., & El-Hawary, M. E. (2012, March). Optimal dynamic economic dispatch including renewable energy source using artificial bee colony algorithm. In 2012 IEEE International Systems Conference SysCon 2012 (pp. 1-6). IEEE.
10. Deb, S., Houssein, E. H., Said, M., & Abdelminaam, D. S. (2021). Performance of turbulent flow of water optimization on economic load dispatch problem. *IEEE Access*, 9, 77882-7789
11. Kaur, A., Singh, L., & Dhillon, J. S. (2022). Modified Krill Herd Algorithm for constrained economic load dispatch problem. *International Journal of Ambient Energy*, 43(1), 4332-4342
12. Al-Betar, M. A., Awadallah, M. A., Zitar, R. A., & Assaleh, K. (2023). Economic load dispatch using memetic sine cosine algorithm. *Journal of Ambient Intelligence and Humanized Computing*, 14(9), 11685-11713.
13. Kusuma, P. D., & Prasasti, A. L. (2024). Stochastic Shaking Algorithm: A New Swarm-Based Metaheuristic and Its Implementation in Economic Load Dispatch Problem. *International Journal of Intelligent Engineering & Systems*, 17(3)
14. Ismaeel, A. A., Houssein, E. H., Khafaga, D. S., Abdullah Aldakheel, E., AbdElrazek, A. S., & Said, M. (2023). Performance of osprey optimization algorithm for solving economic load dispatch problem. *Mathematics*, 11(19), 4107.
15. Yu, J., Kim, C. H., & Rhee, S. B. (2020). Clustering cuckoo search optimization for economic load dispatch problem. *Neural Computing and Applications*, 32(22), 16951-16969.
16. Potfode, A., & Bhongade, S. (2022). Economic Load Dispatch of Renewable Energy Integrated System Using JayaAlgorithm. *Journal of Operation and Automation in Power Engineering*, 10(1), 1-12
17. Keswani, R., Verma, H. K., & Sharma, S. K. (2020, October). Dynamic economic load dispatch considering renewable energy sources using multiswarm statistical particle swarm optimization. In 2020 IEEE International Conference on Computing, Power and Communication Technologies (GUCON) (pp. 405-410). IEEE.

18. Hazra, S., Pal, T., & Roy, P. K. (2021). Renewable energy based economic emission load dispatch using grasshopper optimization algorithm. In Research anthology on clean energy management and solutions (pp. 869-890). IGI Global.
19. Nguyen, H. D., & Pham, L. H. (2023). Solutions of economic load dispatch problems for hybrid power plants using Dandelion optimizer. *Bulletin of Electrical Engineering and Informatics*, 12(5), 2569-2576.
20. Nagarajan, K., Rajagopalan, A., Angalaeswari, S., Natrayan, L., & Mammo, W. D. (2022). Combined economic emission dispatch of microgrid with the incorporation of renewable energy sources using improved mayfly optimization algorithm. *Computational Intelligence and Neuroscience*, 2022(1), 6461690.
21. Sahoo, A. K., Panigrahi, T. K., Dhiman, G., Singh, K. K., & Singh, A. (2021). Enhanced emperor penguin optimization algorithm for dynamic economic dispatch with renewable energy sources and microgrid. *Journal of Intelligent & Fuzzy Systems*, 40(5), 9041-9058.
22. Wang, X., Chu, S. C., Snášel, V., Shehadeh, H. A., & Pan, J. S. (2023). Five phases algorithm: a novel meta-heuristic algorithm and its application on economic load dispatch problem. *Journal of Internet Technology*, 24(4), 837-848.
23. El-Kenawy, E. S. M., Khodadadi, N., Mirjalili, S., Abdelhamid, A. A., Eid, M. M., & Ibrahim, A. (2024). Greylag goose optimization: nature-inspired optimization algorithm. *Expert Systems with Applications*, 238, 122147.
24. Al-Betar, M. A., Awadallah, M. A., Braik, M. S., Makhadmeh, S., & Doush, I. A. (2024). Elk herd optimizer: a novel nature-inspired metaheuristic algorithm. *Artificial Intelligence Review*, 57(3), 48.
25. Ngoc, N. N. T., Arkhincheev, V., & Hoang, H. M. (2026). Starfish Optimization, Sand Cat Swarm Optimization, Weighted Average and Mirage Search Optimization Algorithms for Finding Global Optimal Solutions. *Journal of Advanced Engineering and Computation*, 10(1), 50–68.
26. Tran, M., Tran, C. D., Dinh, B. H., Phan, T. T., Nguyen, T. H. C., Nguyen, H. T., ...& Phan, H. X. (2022). Speed control applying hysteresis current combining sine pulse width modulation for induction motor drive. *Journal of Advanced Engineering and Computation*, 6(1), 45-59.
27. Tran, C. D., Brandstetter, P., Nguyen, M. H. C., Ho, S. D., Pham, P. N., & Dinh, B. H. (2020). An Enhanced Fault Tolerant Control Against Current Sensor Failures in Induction Motor Drive by Applying Space Vector. *Journal of Advanced Engineering and Computation*, 4(1), 51-63.
28. Liu, J., Wang, R., Deng, Y., Huang, X., & Li, Z. (2025). Sharpbelly Fish Optimization Algorithm: A Bio-Inspired Metaheuristic for Complex Engineering. *Biomimetics*, 10(7), 445.
29. Faramarzi, A., Heidarinejad, M., Stephens, B., & Mirjalili, S. (2020). Equilibrium optimizer: A novel optimization algorithm. *Knowledge-based systems*, 191, 105190.
30. Phan, T. T., Tran, T. N., Nguyen, P. T., & Nguyen, D. N. (2025). Reducing the cost of the hybrid system operation by Skill Optimization Algorithm. *Journal of Advanced Engineering and Computation*, 9(2), 58-72.
31. Roy, S., Bhattacharjee, K., & Bhattacharya, A. (2017). A modern approach to solve of economic load dispatch using group leader optimization technique. *International Journal of Energy Optimization and Engineering (IJEEO)*, 6(1), 66-85.
32. Tang, N. A., & Cuong, N. M. D. (2023). Solving the Green Economic Load Dispatch by Applying the Novel Meta-heuristic Algorithm. *Journal of Computing Theories and Applications*, 1(2), 129-139.



33. Spea, S. R. (2025). Cost-effective economic dispatch in large-scale power systems using enhanced manta ray foraging optimization. *Neural Computing and Applications*, 1-38.
34. Van Yen, N., & Chinh, N. T. X. Optimal Power Allocation for Thermal Generators in Solving the Renewable-Based Economic Load Dispatch Using Novel Optimization Algorithms.
35. Jadoun, V. K., Pandey, V. C., Gupta, N., Niazi, K. R., & Swarnkar, A. (2018). Integration of renewable energy sources in dynamic economic load dispatch problem using an improved fireworks algorithm. *IET renewable power generation*, 12(9), 1004-1011.
36. Pham, L. H., Phan, T. T., Phan, K. D. T., & Nguyen, P. H. (2024). Optimizing the Efficiency of Photovoltaic Distributed Generation in the Distribution System. *Journal of Advanced Engineering and Computation*, 8(1), 19-28.

